Supplementary Information:

Thermal-responsive activation of engineered bacteria to trigger antitumor immunity post microwave ablation therapy

Yumin Wu[#1], Bo Liu[#1], Yifan Yan[#1], Chuntao Gong[2], Kaiwei Wang[3], Nanhui Liu[1], Yujie Zhu[1], Maoyi Li[1], Chunjie Wang[1], Yizhe Yang[1], Liangzhu Feng*[1], Zhuang Liu*[1]

1, Jiangsu Key Laboratory for Carbon-Based Functional Materials & Devices, Institute of Functional Nano & Soft Materials (FUNSOM), Soochow University, Suzhou, Jiangsu, 215123, China

2, InnoBM Pharmaceuticals, Suzhou, Jiangsu, 215123, China

3, College of Pharmaceutical Sciences, Soochow University, Suzhou, 215123, China

Email: lzfeng@suda.edu.cn, zliu@suda.edu.cn

[#]These authors contributed equally.

.

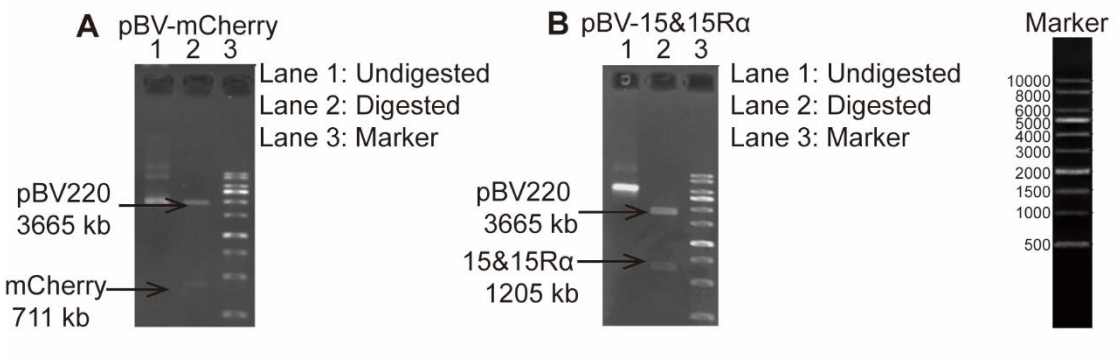

Supplementary Fig. 1. Restriction enzyme digestion maps of plasmids pBV-mCherry (A) and pBV-15&15Rα (B), respectively. This experiment was repeated for three times independently with similar results.

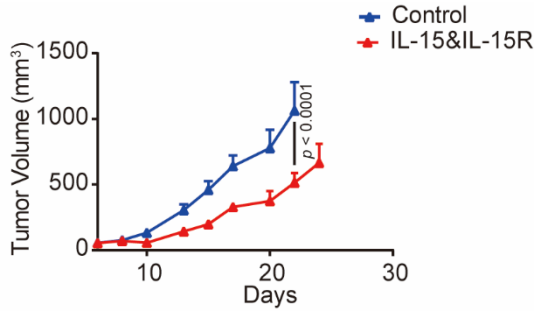

Supplementary Fig. 2. The tumor growth curve following intratumoral injection of IL-15&IL-15Rα in the CT26 tumor-bearing model (n = 5 mice). P value was calculated by two-way ANOVA with Tukey's multiple comparisons. Source data are provided as a Source Data file.

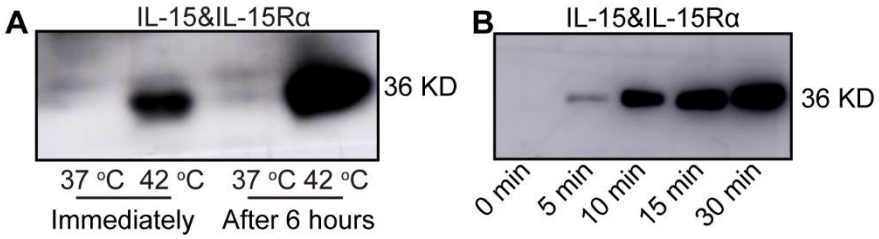

Supplementary Fig. 3. (A) Western blot images of IL-15&IL-15Rα protein in bacterial pellets and induced supernatants of 15&15R@VNP under different conditions, suggesting that the heat-activated bacteria would continuously produce the protein under 37 ℃. (B) Western blot images of IL-15&IL-15Rα protein in bacterial pellets and induced supernatants of 15&15R@VNP under 42°C for different durations. This experiment was repeated for three times independently with similar results.

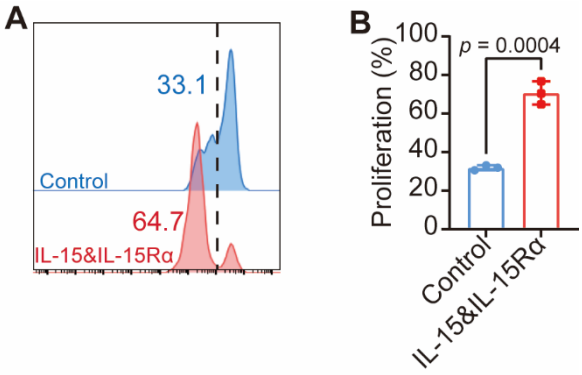

Supplementary Fig. 4. Flow cytometry analysis (A) and percentage (B) of proliferating T cells under different stimulation. Data in the figure were represented as the mean ± SD. P value was calculated by the two-tailed Student's *t-test* (n = 3 samples). Source data are provided as a Source Data file.

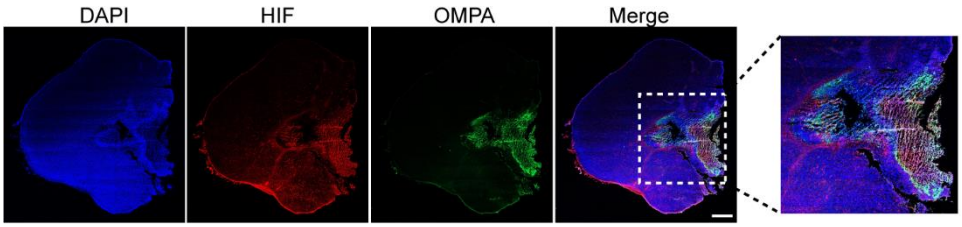

Supplementary Fig. 5. Immunofluorescence staining of whole tumor slices from non-hypoxic region and hypoxic regio. DAPI stands for the nuclei of tumor cells, red for HIF-1α highly expressed cells and green for OMPA-stained salmonella typhimurium. This experiment was repeated for three times independently with similar results. The scale bar was 1000 μm.

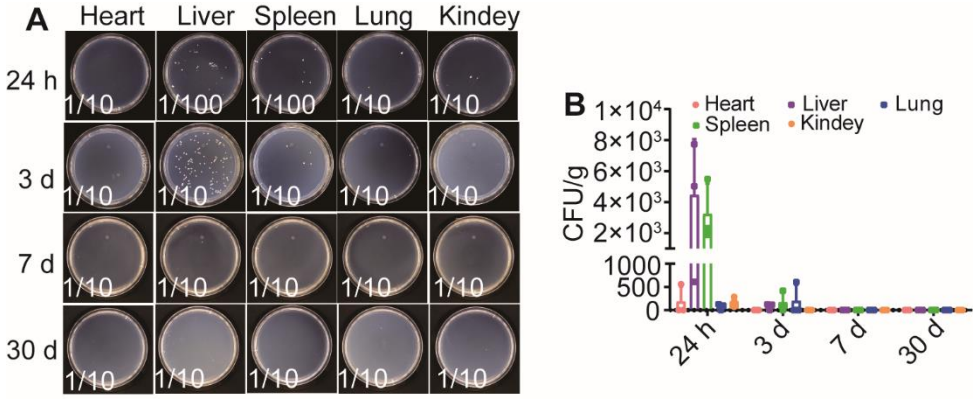

Supplementary Fig. 6. Representative photographs (A) and quantification (B) of bacterial colonization in major organs of healthy mice at different time points after intravenous administration of engineered bacteria (n = 3 mice). Source data are provided as a Source Data file.

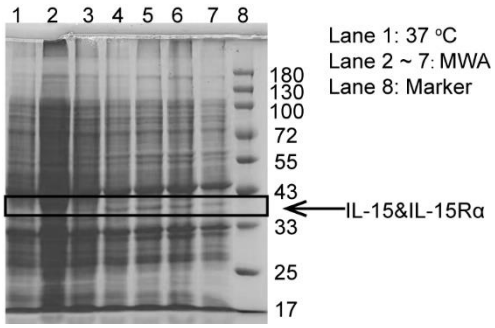

Supplementary Fig. 7. SDS-PAGE images of IL-15&IL-15Rα protein in bacterial pellets and induced supernatants of 15&15R@VNP under MWA treatment. This experiment was repeated for three times independently with similar results.

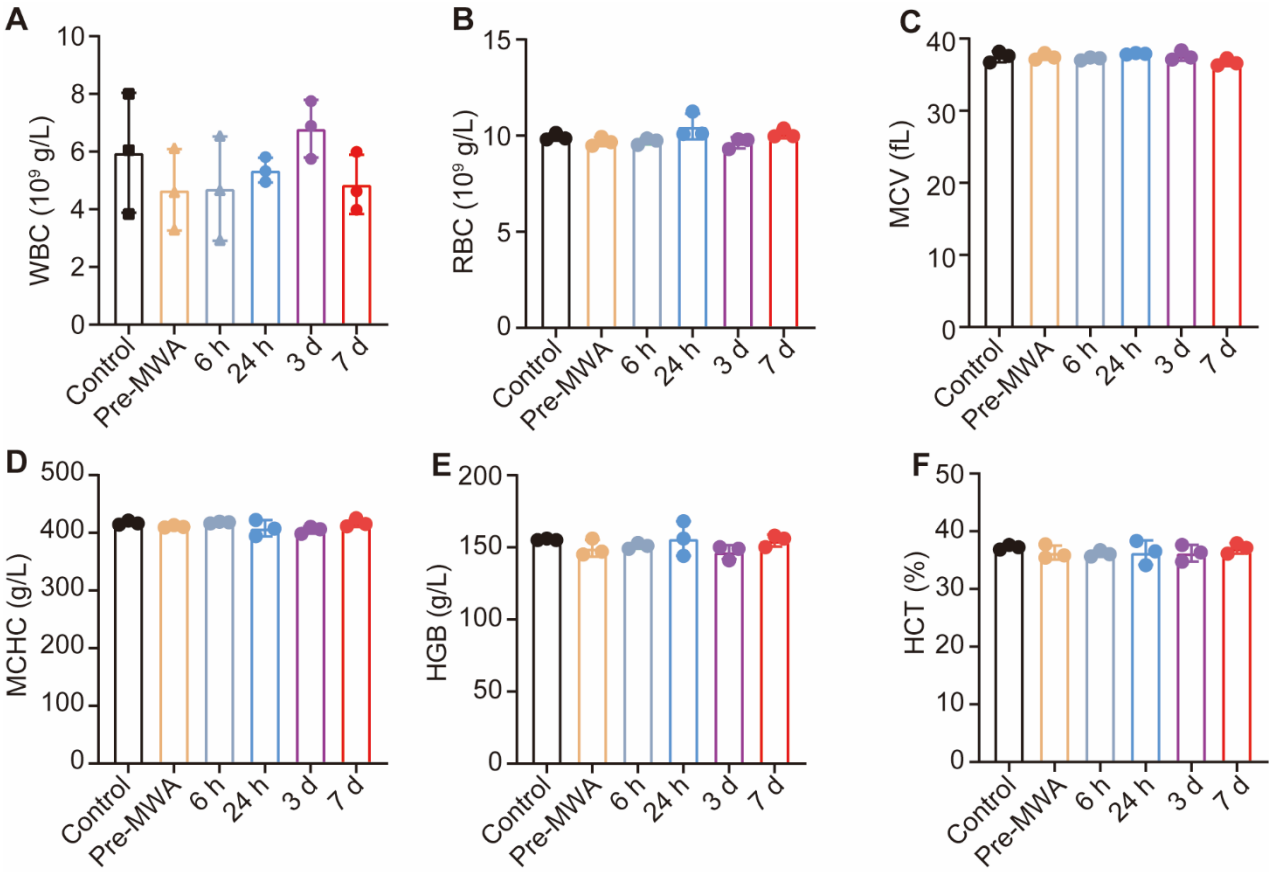

Supplementary Fig. 8. Complete blood panel analysis of mice treated with 15&15R@VNP at different time points following MWA. (A) white blood cells (WBC), (B) red blood cells (RBC), (C) mean corpuscular volume (MCV), (D) mean corpuscular hemoglobin concentration (MCHC), (E) hemoglobin (HGB), (F) hematocrit (HCT) (n = 3 mice). Source data are provided as a Source Data file.

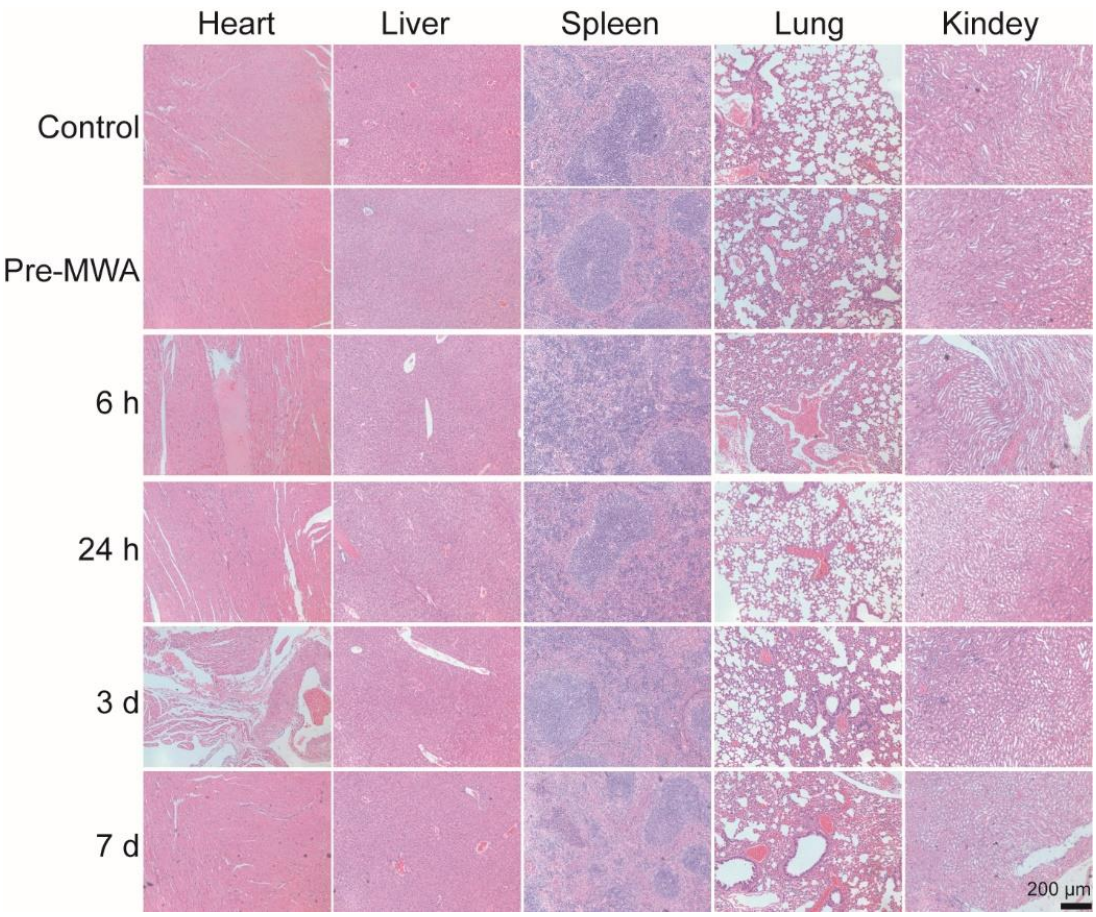

Supplementary Fig. 9. Representative H&E staining images of various organs of mice treated with 15&15R@VNP at different time points following MWA (n = 3 mice). The scale bar was 200 μm.

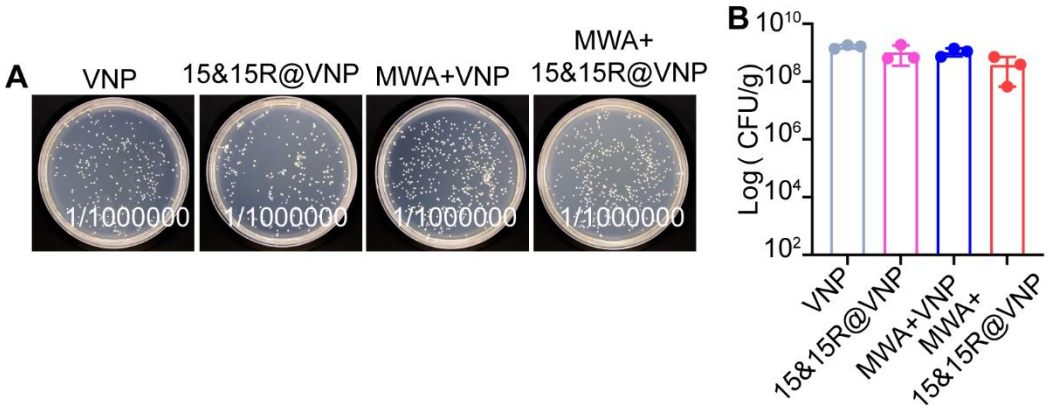

Supplementary Fig. 10. Representative photographs (A) and quantification (B) of bacterial colonization in tumor tissues post different treatments as indicated (n = 3 mice). Source data are provided as a Source Data file.

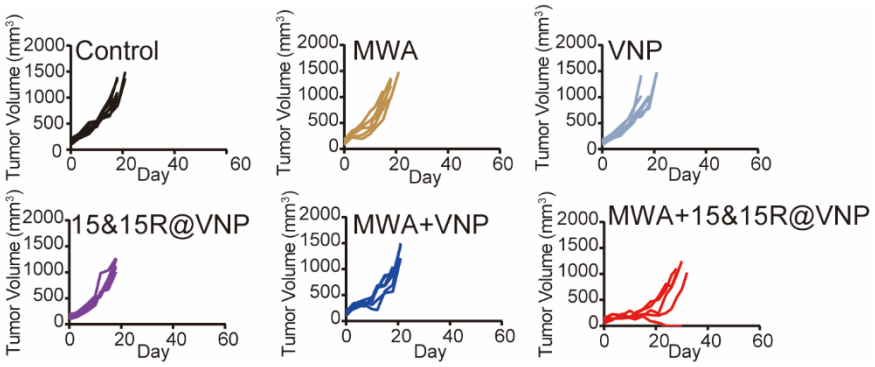

Supplementary Fig. 11. Individual H22 tumor growth curves of mice after different treatments as indicated control group (n = 7 mice), MWA, VNP, 15&15R@VNP, and MWA+15&15R@VNP groups (n = 6 mice), MWA+VNP group (n = 5 mice). Source data are provided as a Source Data file.

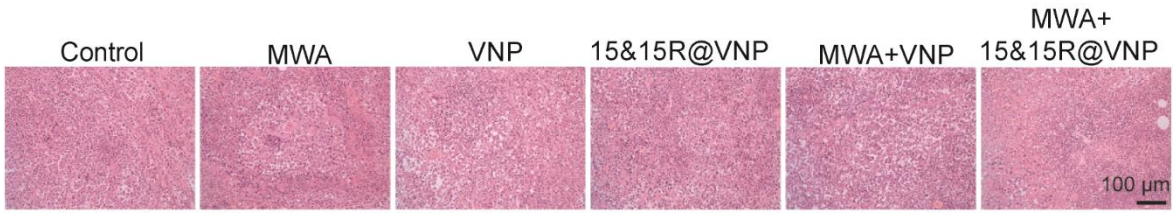

Supplementary Fig. 12. Representative H&E staining images of tumors of mice treated as indicated (n = 3 mice). The scale bar was 100 μm.

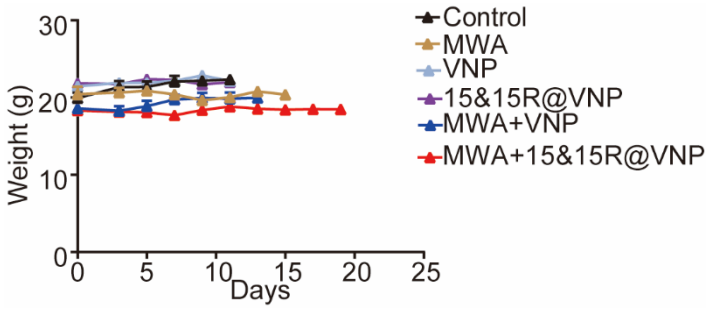

Supplementary Fig. 13. Average body weights of CT26-bearing mice with various treatments as indicated (group control, VNP, 15&15R@VNP, and MWA+15&15R@VNP (n = 6 mice), group MWA and MWA+VNP (n = 5 mice)). Source data are provided as a Source Data file.

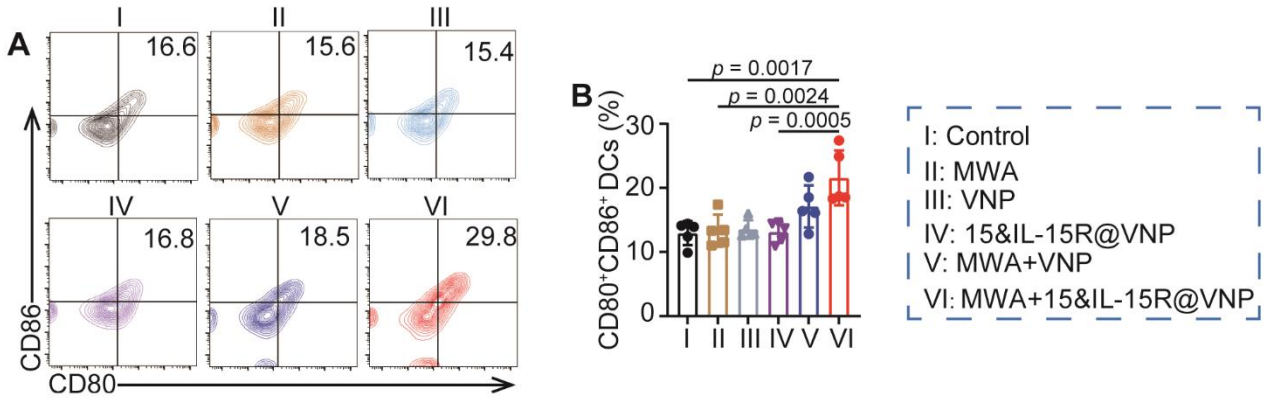

Supplementary Fig. 14. Flow cytometry analysis (A) and percentage (B) of mature DCs in TDLNs of mice post different treatments as indicated. Data in the figure were represented as the mean ± SD. *P* values were calculated by the one-way ANOVA, $n = 5$ mice. Source data are provided as a Source Data file.

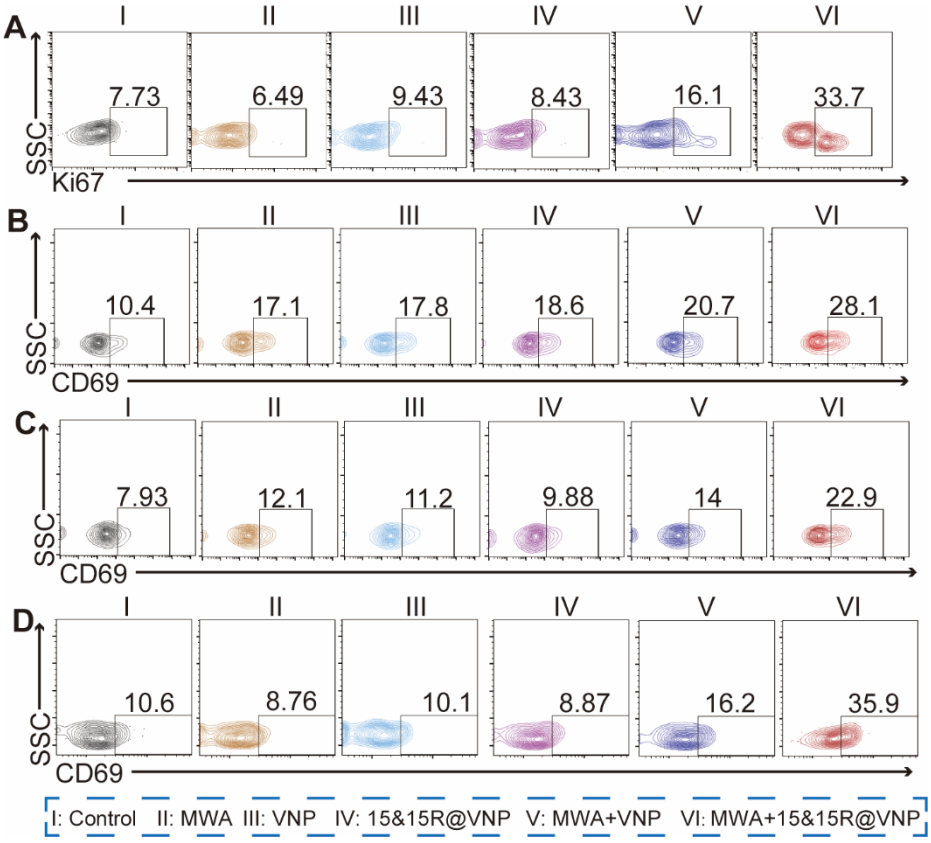

Supplementary Fig. 15. Flow cytometry analysis of $Ki67^+$ T cells (A), $CD69^+$ T cells (B), $CD69^+CD8^+$T cells (C), and $CD69^+$ NK cells (D) in Fig. 5.

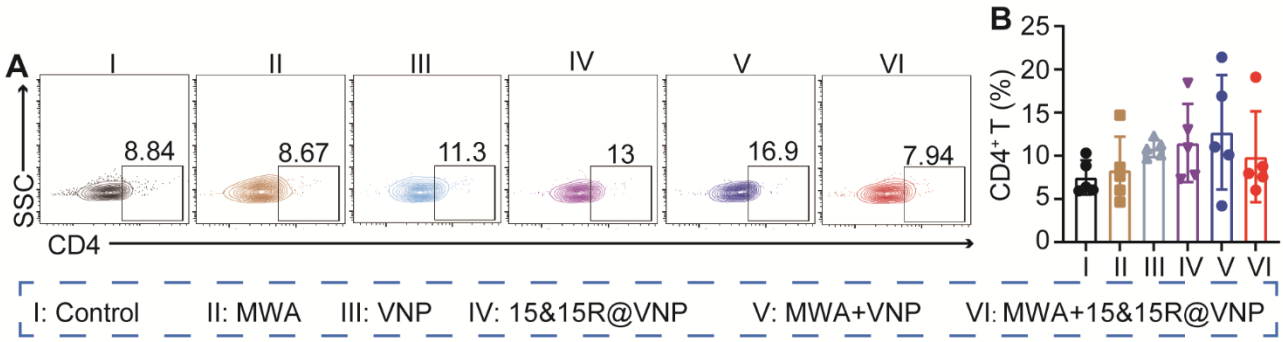

Supplementary Fig. 16. Flow cytometry analysis (A) and percentage (B) of $CD4^+$ T cells inside the tumors after various treatments as indicated. Data in the figure were represented as the mean ± SD, *n* = 5 mice. Source data are provided as a Source Data file.

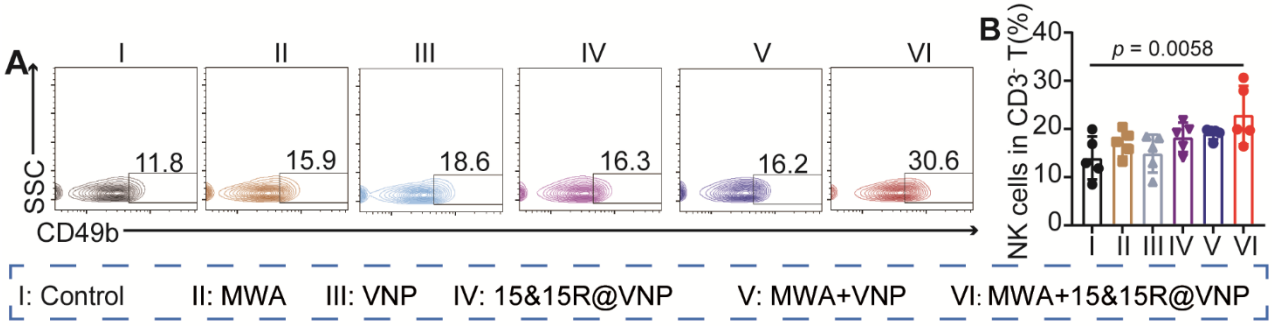

Supplementary Fig. 17. Flow cytometry analysis (A) and percentage (B) of NK cells inside the tumors of mice post different treatments as indicated. Data in the figure were represented as the mean ± SD. *P* value was calculated by the one-way ANOVA, *n* = 5 mice. Source data are provided as a Source Data file.

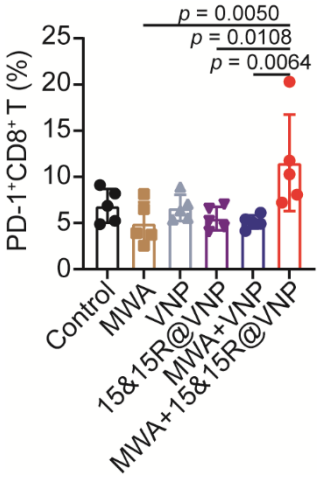

Supplementary Fig. 18. Percentage of $PD\text{-}1^+CD8^+$ T cells inside the tumors after various treatments

as indicated. Data in the figure were represented as the mean ± SD. *P* values were calculated by the one-way ANOVA, *n* = 5 mice. Source data are provided as a Source Data file.

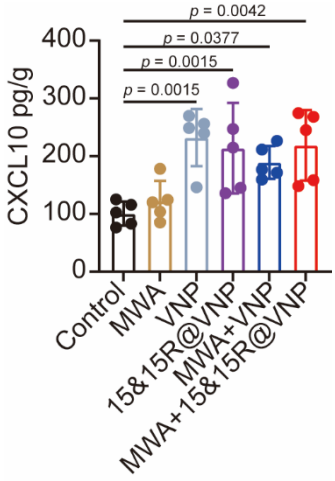

Supplementary Fig. 19. The level of CXCL10 inside the tumors after various treatments is indicated. Data in the figure were represented as the mean ± SD, *p* values were calculated by the one-way ANOVA, *n* = 5 mice. Source data are provided as a Source Data file.

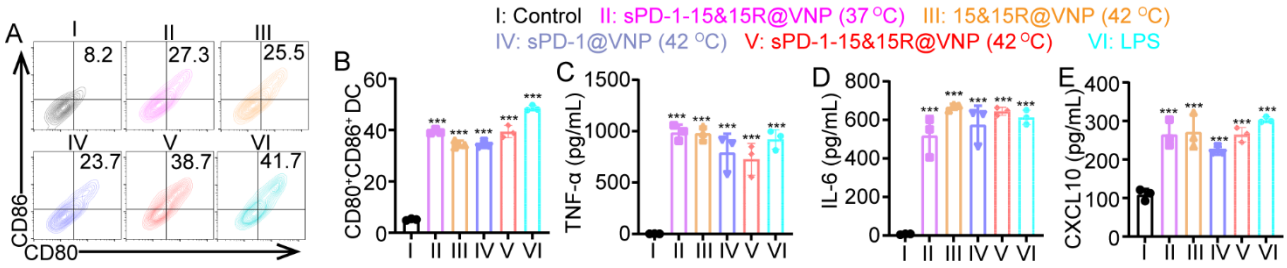

Supplementary Fig. 20. Flow cytometry analysis (A) and percentage (B) of mature BMDCs post different treatments as indicated. (C-E) Secretion levels of TNF-α (C), IL-6 (D) and CXCL10 (E) by BMDCs under different treatments. *P* values were calculated by the one-way ANOVA, *n* = 3 samples, all ***$p<0.00001$. Source data are provided as a Source Data file.

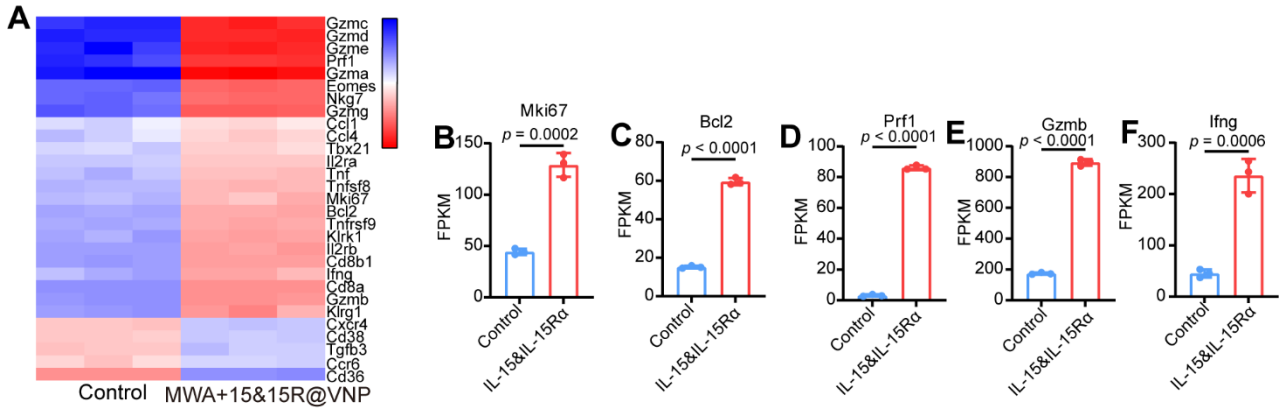

Supplementary Fig. 21. (A) Heatmap of genes involved in T cell proliferation, activation, and cytotoxic activity under different treatments. (B-F) Gene expression levels of Mki67 (B), Bcl2 (C), Prf1 (D), Gzmb (E), Ifng (F). *P* values were calculated by the two-tailed Student's *t-test*, $n = 3$ samples. Source data are provided as a Source Data file.

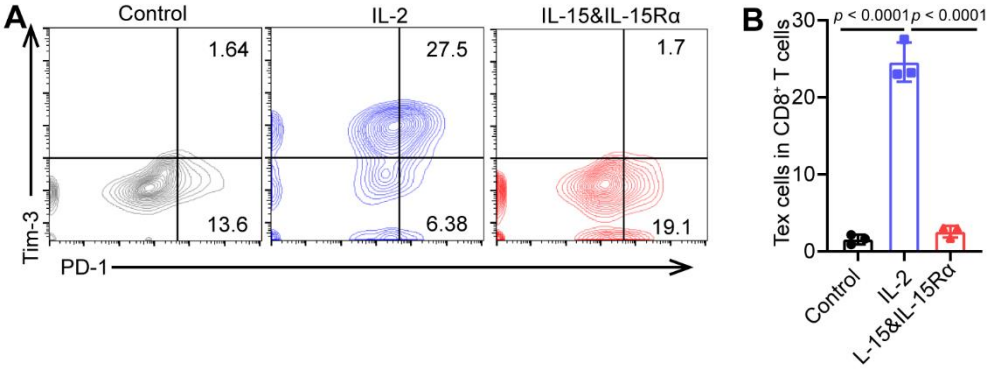

Supplementary Fig. 22. The percentage of Tex cells in $CD8^+$ T cells under different treatments. *P* values were calculated by the one-way ANOVA, $n = 3$ samples. Source data are provided as a Source Data file.

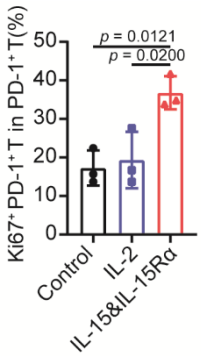

Supplementary Fig. 23. The percentage of $Ki67^+PD\text{-}1^+$ T cells in $PD\text{-}1^+$ T cells under different treatments. *P* values were calculated by the one-way ANOVA, $n = 3$ samples. Source data are

provided as a Source Data file.

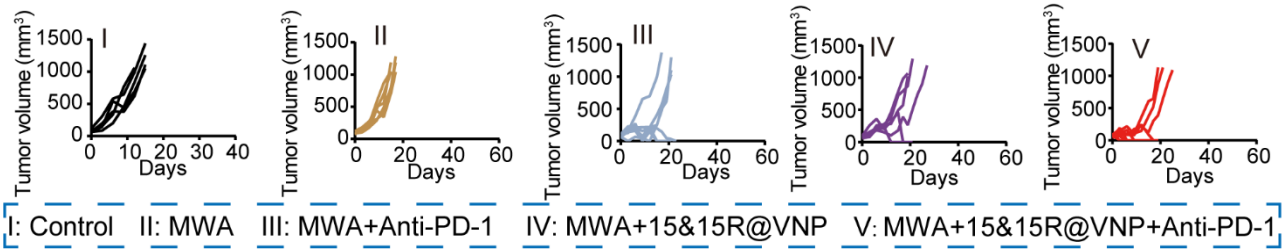

Supplementary Fig. 24. Individual tumor growth curves of CT26 tumor-bearing mice after different treatments as indicated (group I, II, and IV ($n = 6$ mice), group III and V ($n = 7$ mice)). Source data are provided as a Source Data file.

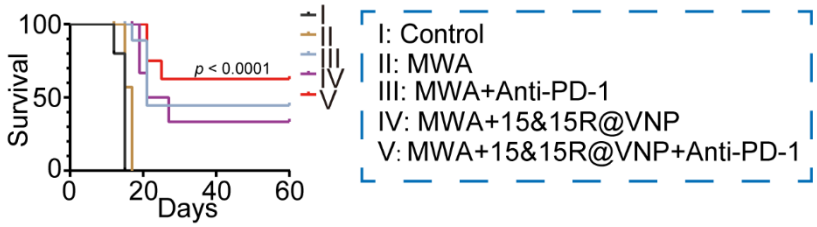

Supplementary Fig. 25. Corresponding mobility-free survival rate of CT26 tumor-bearing mice after different treatments as indicated (group I, II, and IV ($n = 6$ mice), group III and V ($n = 7$ mice)). *P* value was calculated by the log-rank test. Source data are provided as a Source Data file.

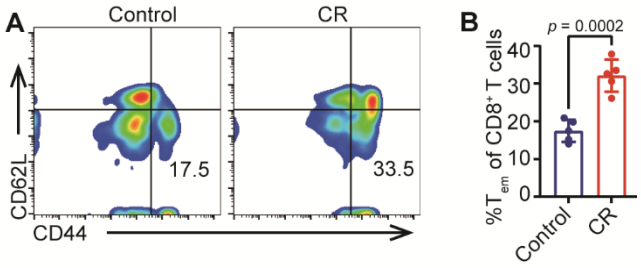

Supplementary Fig. 26. The proportion of T_{em} ($CD45^+CD3^+CD8^+CD44^+CD62L^-$) in the blood of cured mice. *P* value was calculated by the two-tailed Student's *t-test*, $n = 5$ mice. Source data are provided as a Source Data file.

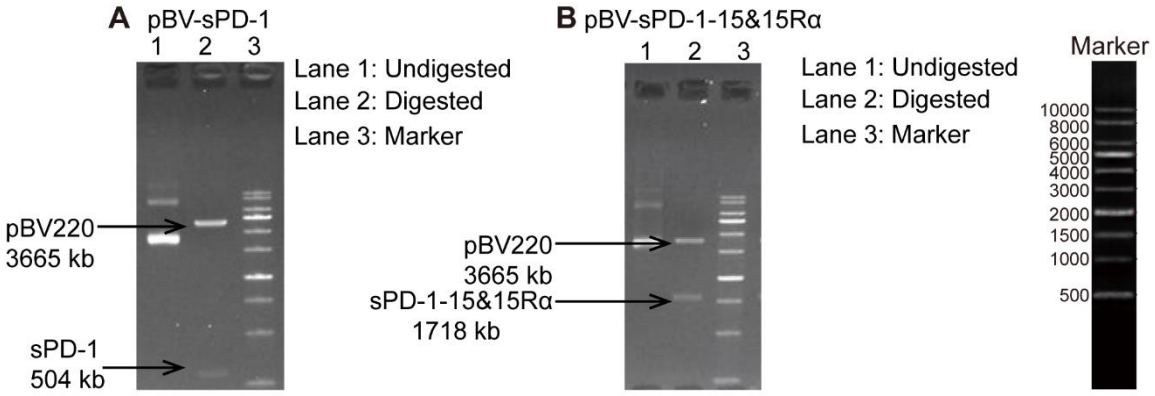

Supplementary Fig. 27. Restriction enzyme digestion maps of plasmids pBV-sPD-1 (A) and pBV-sPD-1-15&15R. This experiment was repeated for three times independently with similar results.

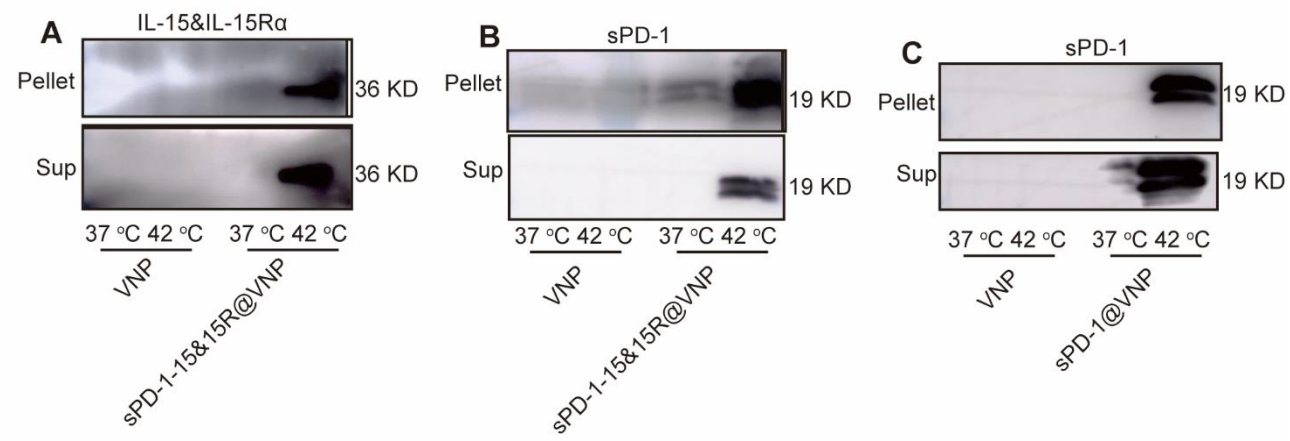

Supplementary Fig. 28. Western blot images of IL-15&IL-15Rα and sPD-1 protein in bacterial pellets and induced supernatants of sPD-1-15&15Rα@VNP (A&B) and sPD-1 protein in bacterial pellets and induced supernatants of sPD-1@VNP (C) under different temperature conditions. This experiment was repeated for three times independently with similar results.

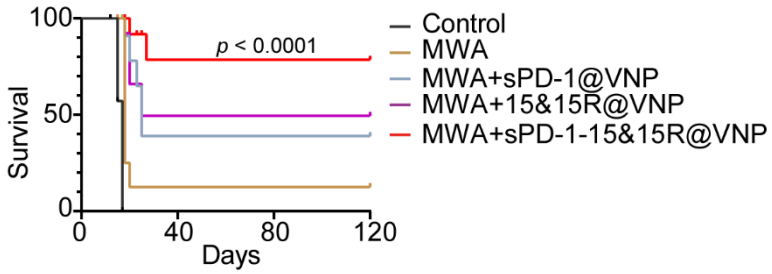

Supplementary Fig. 29. Corresponding mobility-free survival rate of CT26 tumor-bearing mice after different treatments as indicated (group control and MWA+15&15R@VNP ($n = 7$ mice), group MWA, MWA+sPD-1@VNP, and MWA+ sPD-1-15&15R@VNP ($n = 8$ mice)). *P* value was calculated by the

log-rank test. Source data are provided as a Source Data file.

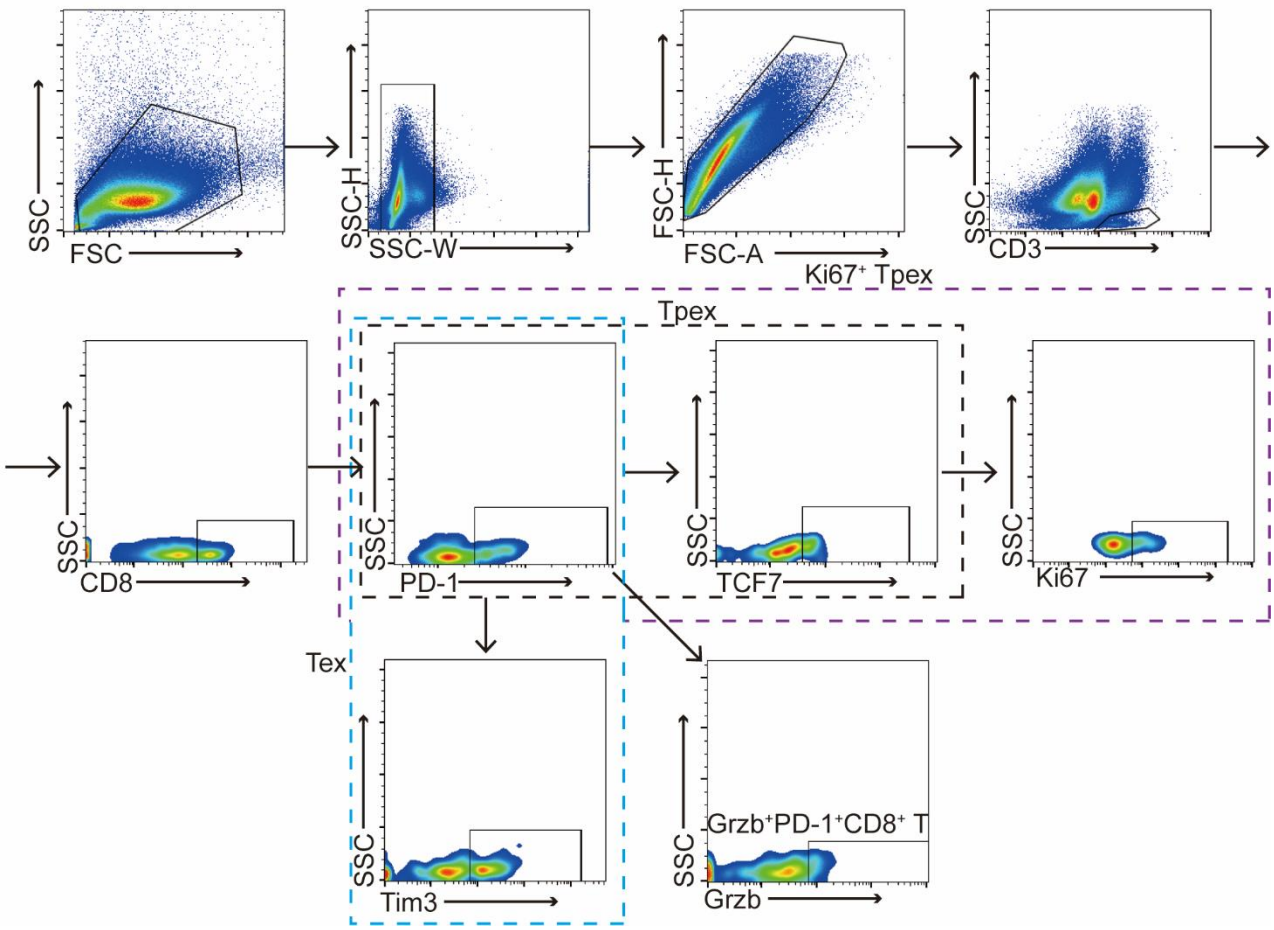

Supplementary Fig. 30. Flow cytometric analysis of Tpex, Ki67^{+} Tpex, Tex, and Grzb^{+}PD-1^{+}CD8^{+} T cells in Fig. 7.

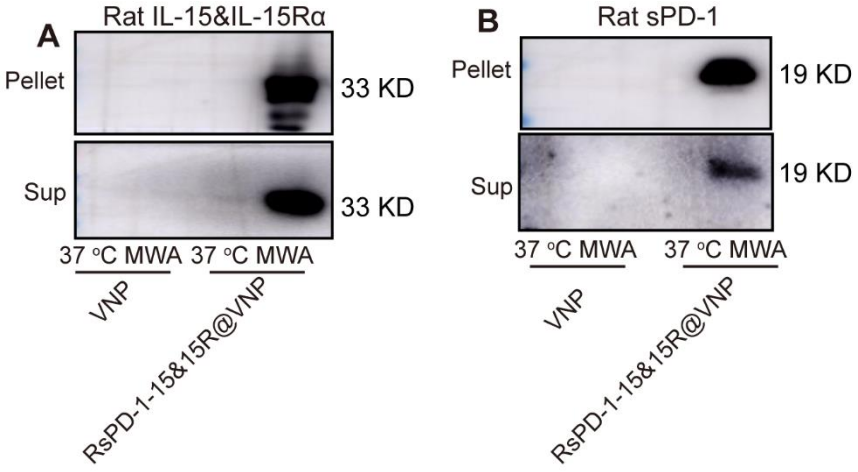

Supplementary Fig. 31. Western blot images of rat IL-15&IL-15Rα (A) and rat sPD-1 (B) protein in bacterial pellets and induced supernatants of sPD-1-15&15Rα@VNP under different temperature conditions. This experiment was repeated for three times independently with similar results.

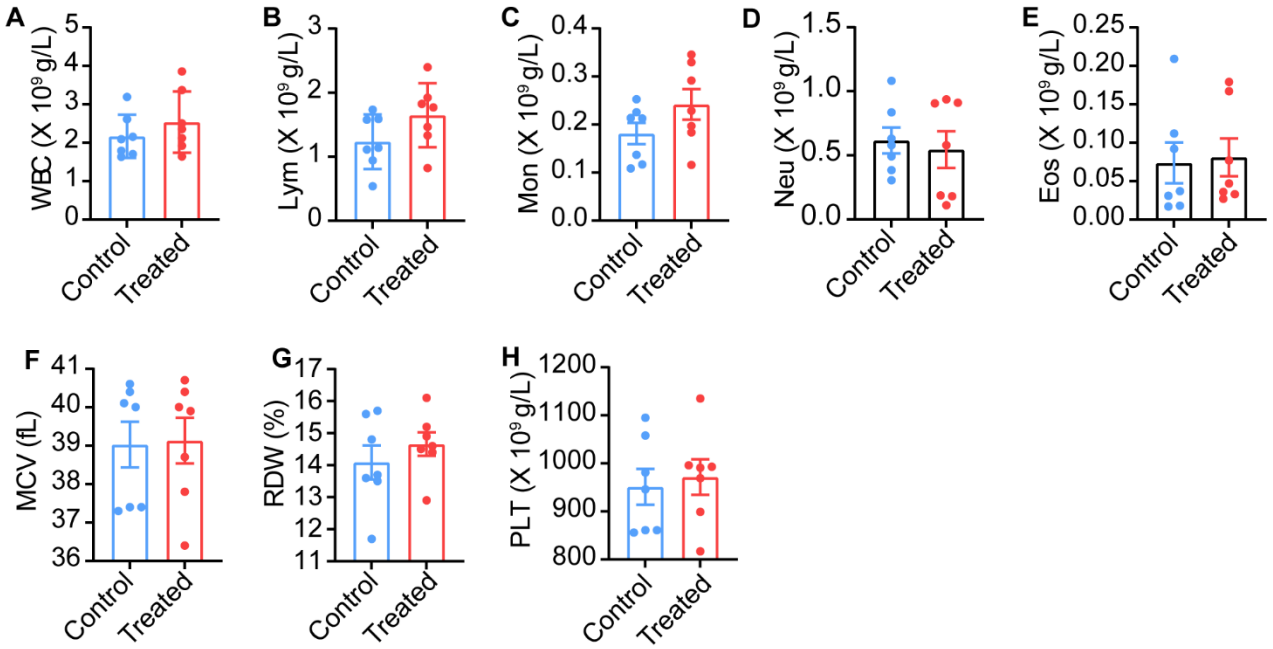

Supplementary Fig. 32. The measured parameters included white blood cells (WBC, A), lymphocyte (Lym, B), monocytes (Mon, C), neutrophil (Neu, D), eosinophil (Eos, E), mean corpuscular volume (MCV, F), red blood cell distribution width, (RDW, G) and blood platelet (PLT, H) collected from these mice at day 30. (M) Generation of red cells in bone marrow. (N&O) Representative FACS profiles (N) and analysis. $N = 7$ mice. Source data are provided as a Source Data file.

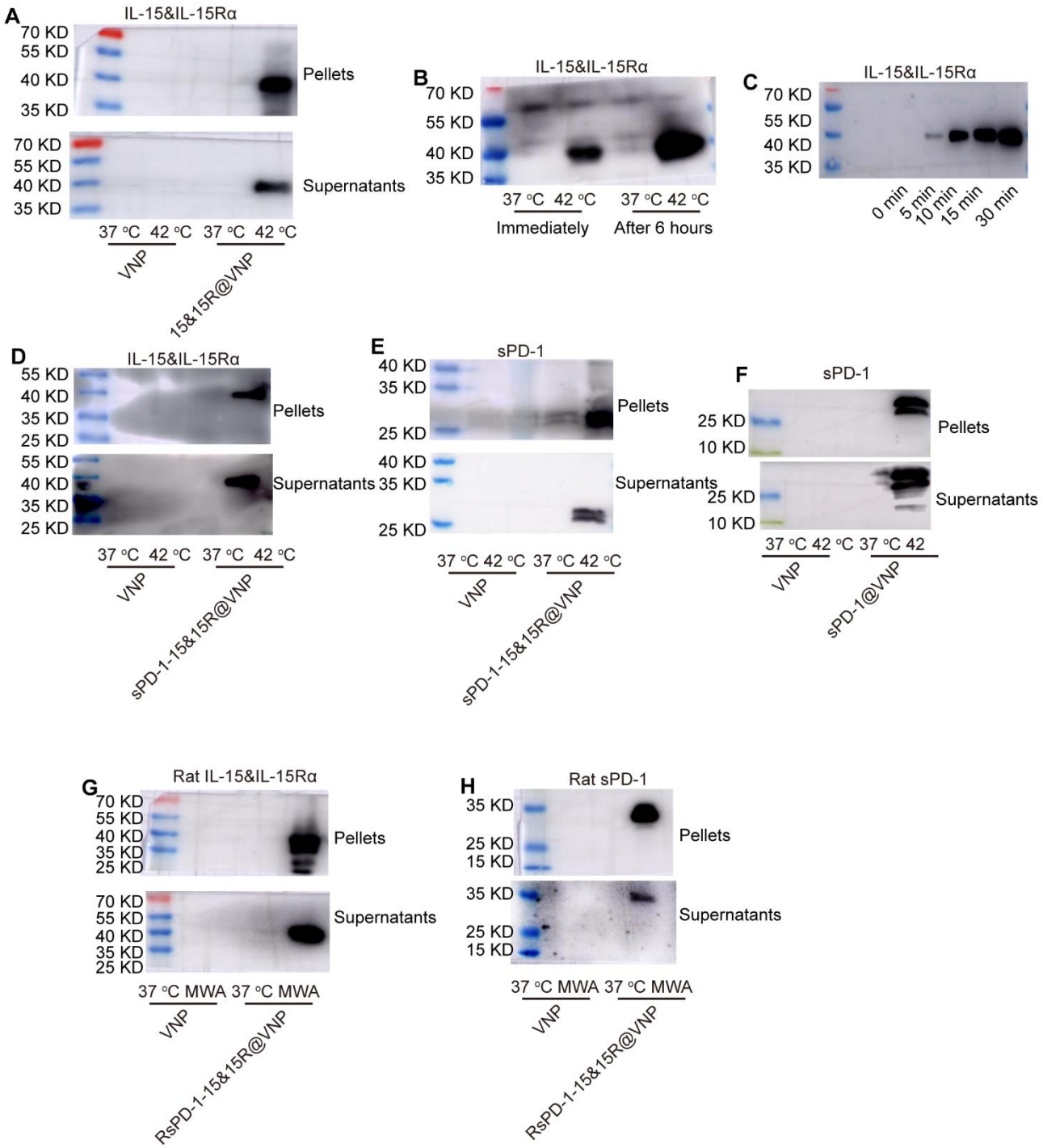

Supplementary Fig. 33. The unprocessed western blot images for Fig. 2L (A), Supplementary Fig. 3A (B), Supplementary Fig. 3B (C), Supplementary Fig. 28A (D), Supplementary Fig. 28A (E), Supplementary Fig. 28A (F), Supplementary Fig. 31A (G), Supplementary Fig. 31B (H).